

This article was downloaded by: [Renmin University of China]

On: 13 October 2013, At: 10:51

Publisher: Taylor & Francis

Informa Ltd Registered in England and Wales Registered Number: 1072954 Registered office: Mortimer House, 37-41 Mortimer Street, London W1T 3JH, UK



## Journal of Coordination Chemistry

Publication details, including instructions for authors and subscription information:

<http://www.tandfonline.com/loi/gcoo20>

### Preparation, crystal structure and luminescence of lanthanide coordination polymers with 2,2'-dimethyl-4,4'-bipyridine-N,N'-dioxide

Jing Xu<sup>a</sup> & Min-Dong Chen<sup>a</sup>

<sup>a</sup> Key Laboratory of Atmospheric Environment Monitoring And Pollution Control, School of Environment Science and Technology, Nanjing University of Information Science and Technology, Nanjing, China

Accepted author version posted online: 21 Jan 2013. Published online: 20 Feb 2013.

To cite this article: Jing Xu & Min-Dong Chen (2013) Preparation, crystal structure and luminescence of lanthanide coordination polymers with 2,2'-dimethyl-4,4'-bipyridine-N,N'-dioxide, Journal of Coordination Chemistry, 66:3, 509-519, DOI: [10.1080/00958972.2012.762975](http://dx.doi.org/10.1080/00958972.2012.762975)

To link to this article: <http://dx.doi.org/10.1080/00958972.2012.762975>

PLEASE SCROLL DOWN FOR ARTICLE

Taylor & Francis makes every effort to ensure the accuracy of all the information (the "Content") contained in the publications on our platform. However, Taylor & Francis, our agents, and our licensors make no representations or warranties whatsoever as to the accuracy, completeness, or suitability for any purpose of the Content. Any opinions and views expressed in this publication are the opinions and views of the authors, and are not the views of or endorsed by Taylor & Francis. The accuracy of the Content should not be relied upon and should be independently verified with primary sources of information. Taylor and Francis shall not be liable for any losses, actions, claims, proceedings, demands, costs, expenses, damages, and other liabilities whatsoever or howsoever caused arising directly or indirectly in connection with, in relation to or arising out of the use of the Content.

This article may be used for research, teaching, and private study purposes. Any substantial or systematic reproduction, redistribution, reselling, loan, sub-licensing, systematic supply, or distribution in any form to anyone is expressly forbidden. Terms &

Conditions of access and use can be found at <http://www.tandfonline.com/page/terms-and-conditions>

## Preparation, crystal structure and luminescence of lanthanide coordination polymers with 2,2'-dimethyl-4,4'-bipyridine-*N,N'*-dioxide

JING XU\* and MIN-DONG CHEN

Key Laboratory of Atmospheric Environment Monitoring And Pollution Control, School of Environment Science and Technology, Nanjing University of Information Science and Technology, Nanjing, China

(Received 20 January 2012; in final form 20 September 2012)

Four coordination polymers of the bidentate ligand 2,2'-dimethyl-4,4'-bipyridine-*N,N'*-dioxide (L), [La(L)(NO<sub>3</sub>)<sub>3</sub>(H<sub>2</sub>O)]<sub>n</sub> (**1**), {[Gd<sub>2</sub>(L)<sub>3</sub>(NO<sub>3</sub>)<sub>6</sub>·6H<sub>2</sub>O]<sub>n</sub> (**2**), {[Sm(L)<sub>2</sub>(H<sub>2</sub>O)<sub>4</sub>]·3ClO<sub>4</sub>·2L·4H<sub>2</sub>O]<sub>n</sub> (**3**) and {[Nd(L)<sub>2</sub>(H<sub>2</sub>O)<sub>4</sub>]·3ClO<sub>4</sub>·2L·4H<sub>2</sub>O]<sub>n</sub> (**4**) have been synthesized by the diffusing solvent mixture method. Results of X-ray diffraction analysis reveal that **1**, with a Ln/L stoichiometry of 1:1, displays a rare 3-D three-fold interpenetrating diamondoid framework, while **2** has a Ln/L stoichiometry of 1:1.5 and exhibits a polycatenane network with a {8<sup>2</sup>,10} topology and large channels accommodated by water. Complexes **3** and **4**, with Ln/L stoichiometry of 1:2, have 3-D two-fold interpenetrating diamondoid structures and large voids. Nonlinear optical property of **2** and luminescence of **3** were also investigated.

**Keywords:** Lanthanide complex; Diffusion solvent mixture; Metal-organic framework; Nonlinear optical property; Photoluminescence property

### 1. Introduction

Design and synthesis of metal-organic frameworks (MOFs) have interest in materials science as new strategies to achieve solid-functionalized materials with potential applications in catalysis, gas storage, magnetism, and optics [1–6]. Various MOFs with interesting structures and specific topologies such as cage, honeycomb, and interpenetrating networks have been obtained by assembly reactions of transition metal salts with rigid or flexible ligands [7]. Lanthanide ions, with higher coordination numbers and more variable coordination geometries, provide opportunities to develop unique frameworks [8,9]. The unique luminescence properties are advantageous in applications such as fluoroimmunoassays, light-emitting diodes, laser systems, and optical amplification for telecommunications [10–13].

Metal complexes having N-oxide ligands have value as magnetic materials [14–16] and show interesting host-guest chemistry [17]. There are a variety of applications of 4,4'-bipyridine-*N,N'*-dioxide [18–22] in both lanthanide and transition metal complexes. Compared with 4,4'-bipyridine-*N,N'*-dioxide, the bidentate ligand 2,2'-dimethyl-4,4'-bipyridine *N,N'*-dioxide (L) possesses two methyls, increasing steric hindrance. It can also serve as a

\*Corresponding author. Email: 002205@nuist.edu.cn

linear ligand to bridge metal centers forming different networks. For example, twofold V-type connectivity affords 1-D chain, threefold T-type and fourfold square planar connectivities lead to 2-D nets, while fourfold tetrahedral and sixfold octahedral connectivities give 3-D frameworks. L not only presents suitable donors for lanthanides, but its limited steric hindrance offers potential for higher coordination numbers and homoleptic coordination spheres. Herein, we present the syntheses, structures, and luminescence of four lanthanide complexes based on L formulated as  $[\text{La}(\text{L})(\text{NO}_3)_3(\text{H}_2\text{O})]_n$  (**1**),  $\{[\text{Gd}_2(\text{L})_3(\text{NO}_3)_6] \cdot 6\text{H}_2\text{O}\}_n$  (**2**),  $\{[\text{Sm}(\text{L})_2(\text{H}_2\text{O})_4] \cdot 3\text{ClO}_4 \cdot 2\text{L} \cdot 4\text{H}_2\text{O}\}_n$  (**3**), and  $\{[\text{Nd}(\text{L})_2(\text{H}_2\text{O})_4] \cdot 3\text{ClO}_4 \cdot 2\text{L} \cdot 4\text{H}_2\text{O}\}_n$  (**4**), which were obtained by a layering diffusion method.

## 2. Experimental

### 2.1. Materials and methods

All commercially available solvents and starting materials were used as received. FT-IR spectra were recorded on a Bruker Vector22 FT-IR spectrophotometer using KBr disks. Elemental analyzes were obtained on a Perkin-Elmer 240C elemental analyzer. Second-order nonlinear optical (NLO) intensity was estimated by measuring a powder sample of 80–150  $\mu\text{m}$  diameter as a pellet relative to urea. A pulsed Q-switched Nd/YAG laser at a wavelength of 1064 nm was used to generate second-harmonic-generation (SHG) signal. The backscattered SHG light was collected by a spherical concave mirror and passed through a filter that transmits only 532 nm radiation. The luminescence spectra for solid samples were recorded at room temperature on an Aminco Bowman Series 2 spectrophotometer with xenon arc lamp as the light source. In the measurements of the emission and excitation spectra, the pass width was 5.0 nm. Powder X-ray diffraction (XRD) measurements were performed on a Bruker D8 Advance X-ray diffractometer using Cu K $\alpha$  radiation (1.5418 Å), and the X-ray tube was operated at 35 kV and 20 mA. The data were collected in the  $2\theta$  range of 5.00°–60.00° with a step size of 0.02°.

### 2.2. Synthesis of 2,2'-dimethyl-4,4'-bipyridine-*N,N'*-dioxide (L)

About 5.4 g (57.4 mmol) of commercially available  $\text{H}_2\text{O}_2$ /urea adduct and 8.5 g (57.4 mmol) of phthalic anhydride were suspended in  $\text{CH}_2\text{Cl}_2$  (60 mL). After 15 min, 2.3 g (12.8 mmol) of 2,2'-dimethyl-4,4'-bipyridine [23] was added and stirred for 3 days. The resulting suspension was poured into a saturated solution of aqueous  $\text{NaHCO}_3$  (200 mL) and continuously extracted with  $\text{CHCl}_3$ . Removing the solution and recrystallizing from  $\text{H}_2\text{O}$  afforded 2.21 g (yield: 80%). IR (KBr,  $\text{cm}^{-1}$ ): 1257 (s), 1245 (vs) (NO). Anal. Calcd for  $\text{C}_{12}\text{H}_{12}\text{N}_2\text{O}_2$ : C, 66.65%; H, 5.59%; N, 12.95%. Found: C, 66.63%; H, 5.61%; N, 12.96%.

### 2.3. Synthesis of complexes

**2.3.1.  $[\text{La}(\text{L})(\text{NO}_3)_3(\text{H}_2\text{O})]_n$  (**1**).**  $\text{La}(\text{NO}_3)_3 \cdot 6\text{H}_2\text{O}$  (0.05 mmol, 21.6 mg) placed at the bottom of a glass vial was covered with  $\text{CHCl}_3$  (8 mL), over which a solution of L (0.10 mmol, 21.5 mg) in  $\text{CH}_3\text{OH}$  (8 mL) was layered. About two weeks later, the solid

Table 1. Crystallographic data for **1–4**.

Complex	<b>1</b>	<b>2</b>	<b>3</b>	<b>4</b>
Chemical formula	C <sub>12</sub> H <sub>13</sub> N <sub>5</sub> O <sub>12</sub> La	C <sub>36</sub> H <sub>48</sub> N <sub>12</sub> O <sub>30</sub> Gd <sub>2</sub>	C <sub>48</sub> H <sub>56</sub> Cl <sub>3</sub> N <sub>8</sub> O <sub>28</sub> Sm	C <sub>48</sub> H <sub>56</sub> Cl <sub>3</sub> N <sub>8</sub> O <sub>28</sub> Nd
<i>M</i>	558.18	1443.27	1449.65	1443.53
Crystal system	Orthorhombic	Orthorhombic	Monoclinic	Monoclinic
Space group	<i>Pnma</i>	<i>P2<sub>1</sub>2<sub>1</sub>2</i>	<i>C2/c</i>	<i>C2/c</i>
<i>a</i> (Å)	11.0015(8)	19.030(3)	33.813(4)	33.912(2)
<i>b</i> (Å)	22.1926(2)	37.337(6)	23.079(3)	23.1782(2)
<i>c</i> (Å)	7.5027(5)	7.9153(13)	24.287(5)	24.3984(2)
$\beta$ (°)	–	–	134.116(1)	134.02
<i>V</i> (Å <sup>3</sup> )	1831.8(2)	5624.0(16)	13607(4)	13789.6(15)
<i>Z</i>	4	4	8	8
<i>T</i> , K	293	293	293	273
<i>M</i> (Mo <i>K</i> $\alpha$ ), cm <sup>-1</sup>	24.09	24.36	10.63	9.52
<i>D</i> <sub>calcd</sub> (g cm <sup>-3</sup> )	2.024	1.690	1.408	1.383
$\lambda$ (Å)	0.71073	0.71073	0.71073	0.71073
<i>R</i> <sub>int</sub>	0.0776	0.1475	0.0932	0.0883
<i>R</i> <sub>1</sub> [ <i>I</i> > 2 $\sigma$ ( <i>I</i> )] <sup>a</sup>	0.0529	0.0722	0.1308	0.0702
<i>wR</i> <sub>2</sub> [ <i>I</i> > 2 $\sigma$ ( <i>I</i> )] <sup>b</sup>	0.1488	0.1851	0.3479	0.2180

<sup>a</sup>*R*<sub>1</sub> =  $\sum||F_o| - |F_c|| / \sum|F_o|$ . <sup>b</sup>*wR*<sub>2</sub> =  $[\sum w(|F_o|^2 - |F_c|^2) / \sum w(F_o)^2]^{1/2}$ , where  $w = 1/[\sigma^2(F_o^2) + (aP)^2 + bP]$ ,  $P = (F_o^2 + 2F_c^2)/3$ .

metal salts gradually dissolved in the solvent mixture with concomitant formation of colorless block crystals on the wall of the vial. The yield of **1** was 40% based on La. Anal. Calcd for C<sub>12</sub>H<sub>13</sub>N<sub>5</sub>O<sub>12</sub>La (**1**): C, 25.82%; H, 2.35%; N, 12.55%. Found: C, 25.85%; H, 2.31%; N, 12.53%. IR (KBr pellet, cm<sup>-1</sup>): 1637 (m), 1476 (s), 1388 (s), 1317 (m), 1232 (s), 1189 (m), 1036 (s), 840 (s), 730 (m), 566 (m).

**2.3.2. {[Gd<sub>2</sub>(L)<sub>3</sub>(NO<sub>3</sub>)<sub>6</sub>]·6H<sub>2</sub>O}<sub>*n*</sub> (**2**).** Complex **2** was produced by a similar procedure to that for **1** but with Gd(NO<sub>3</sub>)<sub>3</sub>·6H<sub>2</sub>O (0.05 mmol, 22.5 mg) instead of La(NO<sub>3</sub>)<sub>3</sub>·6H<sub>2</sub>O. About two weeks later, colorless block crystals were obtained on the wall of the vial. The yield of **2** was 35% based on Gd. Anal. Calcd for C<sub>36</sub>H<sub>48</sub>N<sub>12</sub>O<sub>30</sub>Gd<sub>2</sub> (**2**): C, 29.96%; H, 3.35%; N, 11.65%. Found: C, 29.92%; H, 3.33%; N, 11.67%. IR (KBr pellet, cm<sup>-1</sup>): 1635 (m), 1478 (s), 1385 (s), 1316 (m), 1230 (s), 1183 (m), 1030 (s), 842 (s), 563 (m).

**2.3.3. {[Sm(L)<sub>2</sub>(H<sub>2</sub>O)<sub>4</sub>]·3ClO<sub>4</sub>·2L·4H<sub>2</sub>O}<sub>*n*</sub> (**3**).** Sm(ClO<sub>4</sub>)<sub>3</sub>·6H<sub>2</sub>O (0.05 mmol, 27.8 mg) and L (0.20 mmol, 43.0 mg) were separately dissolved in CH<sub>3</sub>OH (4 mL) and added to two branches of a U-tube, the bottom of which contain CH<sub>2</sub>Cl<sub>2</sub> (6 mL) as a solvent buffer. Yellow block crystals appear at the interface between CH<sub>2</sub>Cl<sub>2</sub> and the metal salt solution over two weeks. The yield of **3** was 25% based on Sm. Anal. Calcd for C<sub>48</sub>H<sub>56</sub>Cl<sub>3</sub>N<sub>8</sub>O<sub>28</sub>Sm (**3**): C, 39.77%; H, 3.89%; N, 7.73%. Found: C, 39.73%; H, 3.91%; N, 7.75%. IR (KBr pellet, cm<sup>-1</sup>): 1647 (m), 1473 (s), 1385 (s), 1310 (m), 1229 (s), 1184 (m), 1030 (s), 845 (s), 568 (m).

**2.3.4. {[Nd(L)<sub>2</sub>(H<sub>2</sub>O)<sub>4</sub>]·3ClO<sub>4</sub>·2L·4H<sub>2</sub>O}<sub>*n*</sub> (**4**).** Complex **4** was produced by a similar procedure to that for **3** but with Nd(ClO<sub>4</sub>)<sub>3</sub>·6H<sub>2</sub>O (0.05 mmol, 27.5 mg) instead of Sm(ClO<sub>4</sub>)<sub>3</sub>·6H<sub>2</sub>O. Lavender block crystals appear at the interface between CH<sub>2</sub>Cl<sub>2</sub> and the

Table 2. Selected bond lengths (Å) and angles (°) for 1–4.

<b>1<sup>a</sup></b>			
La(1)–O(1)	2.465(5)	La(1)–O(2)#1	2.592(6)
La(1)–O(6)#2	2.528(1)	La(1)–O(7)	2.618(1)
O(6)#2–La(1)–O(2)	67.77(3)	O(1W)–La(1)–O(2)	114.72(2)
O(1)–La(1)–O(5)	140.11(2)	O(6)#2–La(1)–O(5)	75.2(4)
O(7)–La(1)–O(5)	40.9(3)	O(4)–La(1)–O(5)	85.42(2)
O(1)–La(1)–N(2)	70.8(2)	O(1)#1–La(1)–N(2)	142.2(2)
O(6)#2–La(1)–N(2)	90.84(2)	O(1W)–La(1)–N(2)	91.03(2)
O(2)–La(1)–N(2)	24.1(2)	O(2)#1–La(1)–N(2)	135.6(2)
O(7)–La(1)–N(2)	74.86(2)	O(4)#1–La(1)–N(2)	142.3(2)
O(4)–La(1)–N(2)	24.2(2)	O(5)–La(1)–N(2)	74.30(2)
N(2)–La(1)–N(2)#1	147.0(3)		
<b>2<sup>b</sup></b>			
Gd(1)–O(1)	2.289(1)	Gd(1)–O(4)	2.333(8)
Gd(1)–O(3)	2.348(9)	Gd(1)–O(13)	2.460(1)
Gd(1)–O(9)	2.479(1)	Gd(1)–O(10)	2.483(9)
Gd(1)–O(15)	2.485(1)	Gd(1)–O(12)	2.492(9)
Gd(1)–O(8)	2.501(1)	Gd(1)–N(9)	2.892(1)
Gd(1)–N(8)	2.901(1)	Gd(1)–N(7)	2.915(1)
O(3)–Gd(1)–N(9)	82.0(4)	O(13)–Gd(1)–N(9)	25.5(4)
O(9)–Gd(1)–N(9)	157.5(4)	O(10)–Gd(1)–N(9)	95.1(4)
O(15)–Gd(1)–N(9)	25.3(4)	O(12)–Gd(1)–N(9)	99.6(4)
O(13)–Gd(1)–N(8)	72.4(3)	O(9)–Gd(1)–N(8)	84.9(4)
O(2)#1–Gd(2)–O(22)	78.4(3)	O(6)–Gd(2)–O(22)	76.5(3)
O(18)–Gd(2)–O(22)	72.0(4)	O(16)–Gd(2)–O(22)	116.8(4)
O(19)–Gd(2)–O(22)	122.1(3)	O(24)–Gd(2)–O(22)	51.0(3)
O(5)–Gd(2)–O(21)	76.3(4)	O(2)#1–Gd(2)–O(21)	75.9(3)
<b>3<sup>c</sup></b>			
Sm(1)–O(1)	2.312(1)	Sm(1)–O(4)#1	2.318(1)
Sm(1)–O(2)#2	2.365(1)	Sm(1)–O(3)	2.365(1)
O(2)#2–Sm(1)–O(8)	80.9(5)	O(3)–Sm(1)–O(8)	66.0(4)
O(5)–Sm(1)–O(8)	136.1(4)	O(1)–Sm(1)–O(6)	82.3(5)
O(4)#1–Sm(1)–O(6)	68.5(4)	O(2)#2–Sm(1)–O(6)	136.3(4)
O(3)–Sm(1)–O(6)	76.9(5)	O(5)–Sm(1)–O(6)	68.4(4)
O(8)–Sm(1)–O(6)	129.2(5)	O(1)–Sm(1)–O(7)	67.8(4)
O(4)#1–Sm(1)–O(7)	79.8(5)	O(2)#2–Sm(1)–O(7)	77.9(5)
O(3)–Sm(1)–O(7)	134.5(4)	O(5)–Sm(1)–O(7)	129.7(5)
O(8)–Sm(1)–O(7)	68.6(4)	O(6)–Sm(1)–O(7)	137.8(5)
<b>4<sup>d</sup></b>			
Nd(1)–O(3)	2.344(6)	Nd(1)–O(2)#1	2.348(6)
Nd(1)–O(1)	2.411(5)	Nd(1)–O(4)#2	2.434(6)
Nd(1)–O(5)	2.485(6)	Nd(1)–O(7)	2.492(5)
Nd(1)–O(8)	2.508(6)	Nd(1)–O(6)	2.511(6)
O(3)–Nd(1)–O(2)#1	84.8(2)	O(3)–Nd(1)–O(1)	156.2(2)
O(2A) #1–Nd(1)–O(1)	95.9(2)	O(3)–Nd(1)–O(4)#2	95.0(2)
O(2)#1–Nd(1)–O(4)#2	157.8(2)	O(1)–Nd(1)–O(4)#2	93.1(2)
O(3)–Nd(1)–O(5)	135.6(2)	O(2)#1–Nd(1)–O(5)	79.6(2)
O(1)–Nd(1)–O(5)	67.43(2)	O(4)#2–Nd(1)–O(5)	85.2(2)
O(2)#1–Nd(1)–O(6)	82.6(2)	O(1)–Nd(1)–O(6)	136.3(2)
O(4)#2–Nd(1)–O(6)	76.8(2)	O(5)–Nd(1)–O(6)	69.4(2)
O(7)–Nd(1)–O(6)	128.5(2)	O(8)–Nd(1)–O(6)	137.6(2)

<sup>a</sup>Symmetry transformations used to generate equivalent atoms: #1:  $x, -y+3/2, z$ , #2:  $x+1/2, y, -z+5/2$ . <sup>b</sup>Symmetry transformations used to generate equivalent atoms: #1:  $x-1/2, -y+3/2, -z+1$ . <sup>c</sup>Symmetry transformations used to generate equivalent atoms: #1:  $x, -y+1, z-1/2$ , #2:  $x+1/2, -y+1/2, z+1/2$ . <sup>d</sup>Symmetry transformations used to generate equivalent atoms: #1:  $x, -y, z+1/2$ , #2:  $x-1/2, -y+1/2, z-1/2$ .

metal salt solution over two weeks. The yield of **4** was 27% based on Nd. Anal. Calcd for C<sub>48</sub>H<sub>56</sub>Cl<sub>3</sub>N<sub>8</sub>O<sub>28</sub>Nd (**3**): C, 39.94%; H, 3.91%; N, 7.76%. Found: C, 39.93%; H, 3.89%;

N, 7.78%. IR (KBr pellet,  $\text{cm}^{-1}$ ): 1639 (m), 1473 (s), 1386 (s), 1308 (m), 1227 (s), 1181 (m), 1032 (s), 840 (s), 560 (m).

#### 2.4. X-ray structure determination

Crystallographic data of **1–3** were collected at 293 K (**4** was collected at 273 K) on a Bruker SMART CCD system equipped with monochromated Mo-K $\alpha$  radiation ( $\lambda = 0.71073 \text{ \AA}$ ) using  $\omega$ - $\phi$  scan technique. The data integration and empirical absorption corrections were carried out by SAINT [24]. The structures were solved by direct methods using SHELXS 97 [25]. All nonhydrogen atoms were refined anisotropically on  $F^2$  by full-matrix least-squares methods [26] and hydrogens (except H1W in **1** and those on  $-\text{CH}_3$  of L in **3**) were generated geometrically and refined isotropically using the riding model. H1W in **1** and those on  $-\text{CH}_3$  of L in **3** were located directly from the Fourier map. H1W in **1** has a site occupancy factor of 0.5. The reported R factors of **3** are a little higher due to disorder of solvent water. Details of the crystal parameters, data collection and refinements for **1–4** are summarized in table 1. Selected bond lengths and angles for **1–4** are listed in table 2.

### 3. Results and discussion

#### 3.1. Preparation of the complexes

The traditional layering method is achieved by putting methanol solution of metal salts over the halogenated solution of the ligand [27–30], with both L and lanthanide salts being soluble in methanol and slightly soluble in  $\text{CHCl}_3$  or  $\text{CH}_2\text{Cl}_2$ . Thus, solid metal salts are put in the bottom of the vessel, then covered by  $\text{CHCl}_3$  or  $\text{CH}_2\text{Cl}_2$  solution, and then finally layered by methanol solution of L.

#### 3.2. Description of the crystal structures

**3.2.1. The crystal structure of 1.** The results of X-ray crystallographic analysis reveal that **1** crystallizes in orthorhombic space group  $Pnma$  (table 1). The asymmetric unit of **1** consists of one La(III), one L, three coordinated nitrates and one coordinated water. As displayed in figure 1(a), each La(III) is nine-coordinate with distorted tricapped trigonal prismatic coordination geometry with a nine-oxygen donor set formed by two oxygens from two different L, four oxygens from two bidentate nitrates, two oxygens from two monodentate nitrates, and one water. The two 2,2'-dimethyl-4,4'-bipyridine- $N,N'$ -dioxide ligands form a "V-type" at La(III) with a  $\text{La}\cdots\text{La}\cdots\text{La}$  angle of  $108.26^\circ$ ; neighboring La(III) centers are connected by a bridging nitrate to form a zigzag ladder (figure 1(b)), with each La(III) connecting four other La(III) ions. When viewed along the  $a$  direction, the structure contains large channels ( $ca. 10 \times 10 \text{ \AA}$ ) as illustrated in figure 1(c); each La(III) is a four-connected node and the network forms a 3-D structure of  $6^6$  topology.

There are large voids in **1** as mentioned previously and interpenetration occurs. There are three individual 3-D **dia** nets interpenetrating due to the large void in the single net (figure 1(d)). Threefold interpenetrating networks based on four-connected centers are

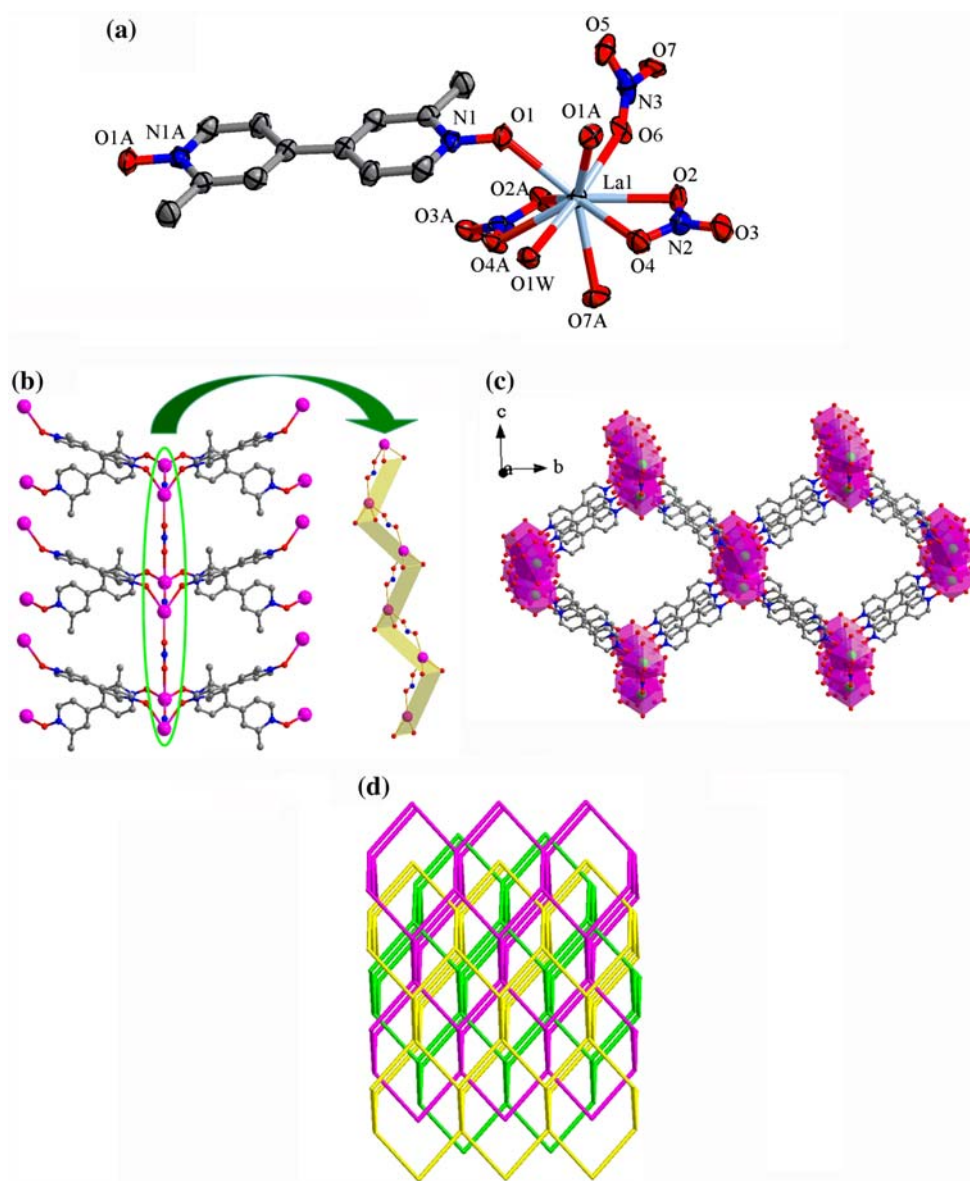


Figure 1. (a) Coordination environment of La(III) in **1** with ellipsoids drawn at 50% probability; hydrogens are omitted for clarity. (b) Neighboring La(III) centers connected by a bridging nitrate form a zigzag ladder. (c) A single fold structure of **1**. (d) 3-D three-fold interpenetrating *dia* topological framework in **1**.

scarce, especially for lanthanide complexes [31], although a few examples of two-fold or four-fold interpenetrating structures have been reported [32,33].

**3.2.2. The crystal structure of 2.** Complex **2** crystallizes in the orthorhombic noncentrosymmetric space group  $P2_12_12$  (table 1). The asymmetric unit of **2** contains two Gd(III), although both are nine-coordinate, the coordination environments slightly differ as depicted



in figure 2(a). The Gd1(III) and Gd2(III) in **2** both have distorted tricapped trigonal prismatic coordination geometry with the three L forming a “T-type” at Gd(III); the remaining coordination sites are occupied by three bidentate nitrates. The difference between Gd1 and Gd2 is the coordination of three nitrates. Three nitrates of Gd1 adopt a “T-joint” structure with two nitrates para: those of Gd2 have a “Y-joint” structure with each nitrate on a different direction. Such connections lead to neutral double-zigzag chains constructed by  $\mu_2$ -connection of L and interlaced connection of Gd1 and Gd2 from the *a* direction (figure 2(b)).

From the *c* direction, **2** has an infinite net structure (figure 2(c)), both Gd1 and Gd2 are 3-connecting nodes, while each L is linear linking two Gd(III) with a Gd–Gd separation from 12.79 to 13.43 Å; thus, it exhibits a 2-D network with  $\{8^2, 10\}$  topology which is seldom reported [34]. The three-connected nodes of the net are equivalent, and each is connected to another node through a direct bond. There are large channels in the single net and interpenetration occurs as shown in figure 2(d); it could well be considered as a polycatenane. There still is free space which is calculated by PLATON analysis as 21.0% (1179.6 Å<sup>3</sup> per unit) filled by water [35].

**3.2.3. The crystal structures of 3 and 4.** To investigate the impact of anions on the structure of the assembly reaction product, Ln(ClO<sub>4</sub>)<sub>3</sub> instead of Ln(NO<sub>3</sub>)<sub>3</sub> was used to react with L. ClO<sub>4</sub><sup>−</sup> does not coordinate with Ln(III), acting only as counteranions to give **3** and **4**. XRD analyzes indicate that **3** and **4** are isomorphous and isostructural (table 1), and thus, only the structure of **3** is taken as an example to describe here. Complex **3** crystallizes in the monoclinic space group *C2/c*, and the asymmetric unit of **3** contains one Sm(III) located at a special position, two L, four coordinated waters, three ClO<sub>4</sub><sup>−</sup>, two uncoordinated L and four free waters. As shown in figure 3(a), each Sm(III) is eight-coordinate by four oxygens of four L and four waters. The coordination geometry of Sm can be described as a distorted dodecahedron with Sm–O bond distances from 2.312(1) to 2.506(1) Å and O–Sm–O bond angles of 66.0(4)°–157.4(5)° (table 2), which are all in the normal range and similar to those observed [36,37]. Among **1–4**, the average Ln–O bond lengths decrease with increasing atomic number of the lanthanide, which reflects the lanthanide contraction.

In **3**, each L is a two-connector linking two Sm(III) using its two oxygens and each Sm(III) is linked to four adjacent metals at distances of 13.407–13.483 Å through four L to form a 3-D four-connected framework structure (figure 3(b)). The topology can be described as **dia** net with the Schläfli symbol of 6<sup>6</sup>. The structure of **3** consists of cationic diamondoid frameworks, two independent **dia** nets interpenetrate within the whole structure as shown in figure 3(c). Large voids form, although it has two-fold interpenetration (figure 3(d)). The effective free volume of **3** calculated by PLATON analysis is 69.1% (9397.1 Å<sup>3</sup> per unit) filled by ClO<sub>4</sub><sup>−</sup>, L and water [35].

### 3.3. NLO property of 2

A noncentrosymmetric structure may have second-order NLO effects, and due to the advantage over pure organic or inorganic compounds, NLO properties of organic–inorganic complexes is of interest [38,39]. Complex **2** crystallizes in the orthorhombic space group *P2<sub>1</sub>2<sub>1</sub>2*, and thus, quasi-Kurtz SHG measurements were studied on powder sample of **2** to confirm acentricity as well as to evaluate its potential application as a second-order NLO material [40]. Preliminary results show the bulk materials of **2** display modest powder SHG activity with a response of approximately 0.6 times that for urea.

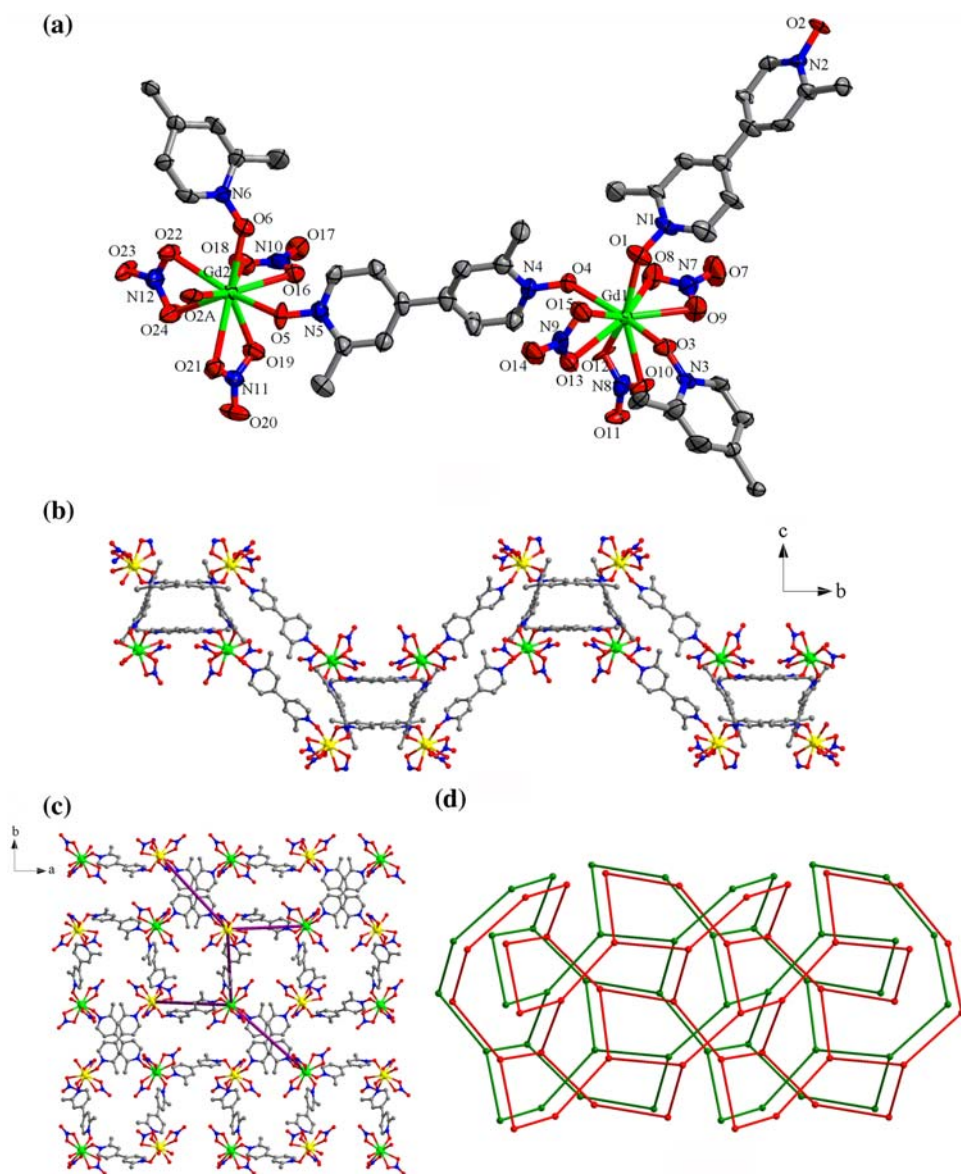


Figure 2. (a) Coordination environment of Gd(III) in **2** with ellipsoids drawn at 50% probability; uncoordinated waters and hydrogens are omitted for clarity. (b) Neutral double-zigzag chains constructed by L along the *a* axis of **2**. (c) Gd1 and Gd2 are 3-connecting nodes in a single 2-D layer from the *c* axis of **2**. (d) Polycatenane of {8<sup>2</sup>,10} topological network in **2**.

### 3.4. Visible luminescent properties

Taking account of the excellent luminescence of lanthanide complexes, solid-state luminescent properties of **1–4** were investigated at room temperature. No detectable luminescence was observed for **1**, **2**, and **4** under the experimental conditions. Complex **3** displays red lumines-

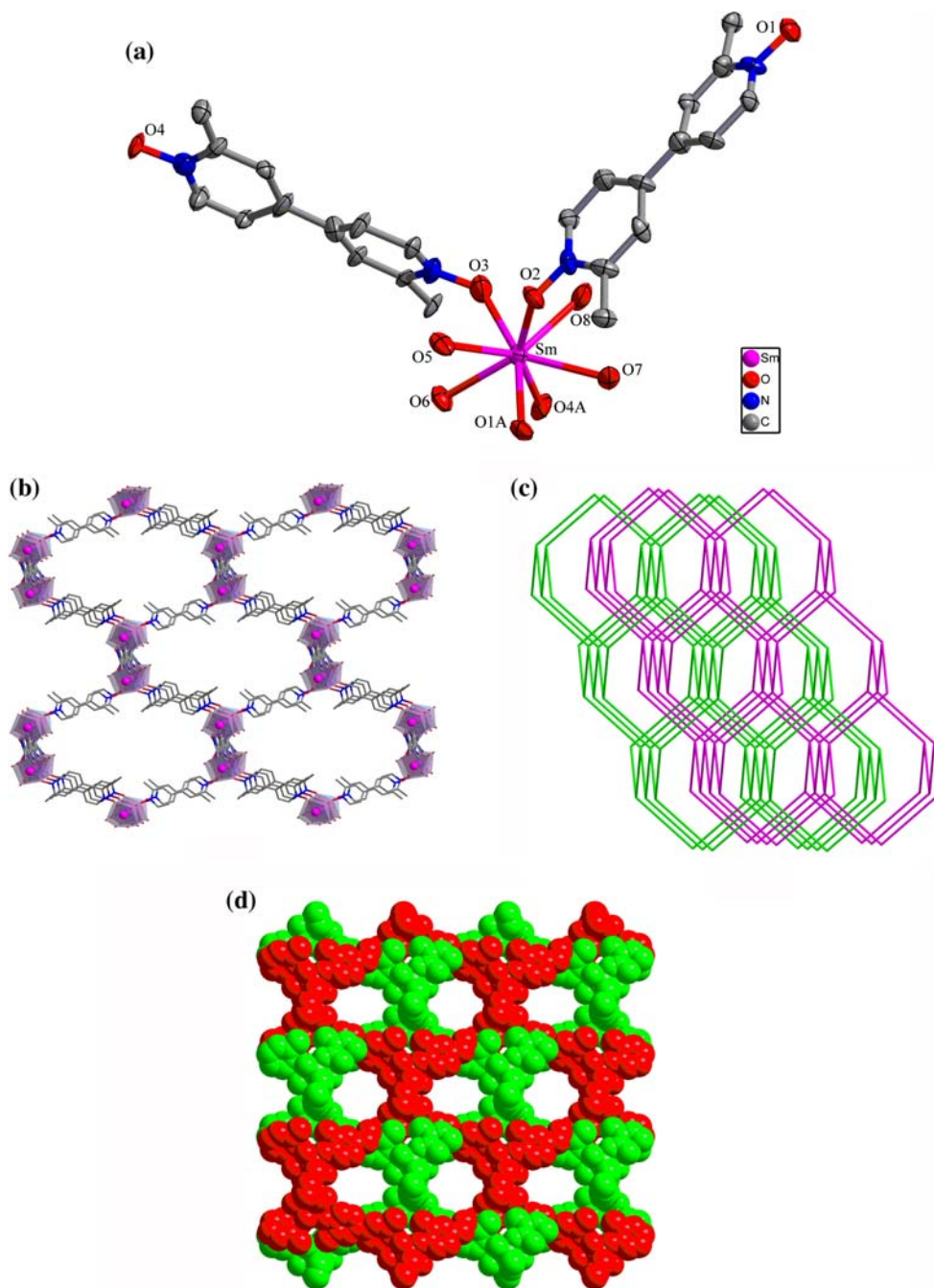


Figure 3. (a) Coordination environment of Sm(III) in **3** with ellipsoids drawn at 50% probability,  $\text{ClO}_4^-$ , uncoordinated L; hydrogens and solvent water are omitted for clarity. (b) A single fold structure of **3**. (c) 3-D two-fold interpenetrating *dia* topological framework in **3**. (d) The space filling mode of a two-fold interpenetrating structure in **3**.

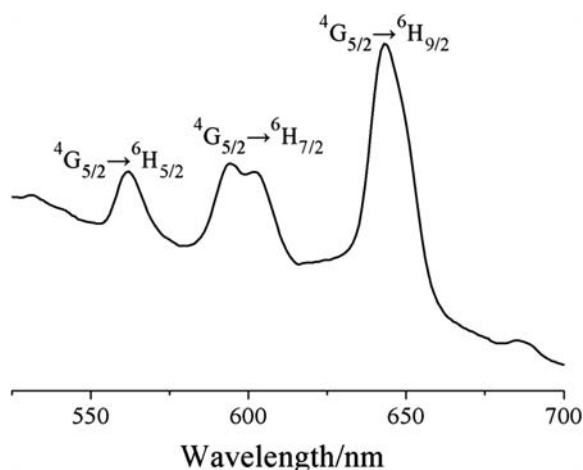


Figure 4. Phosphorescence emission spectra of **3** in the solid state at room temperature.

cence (figure 4) upon excitation at 392 nm with emissions at 561, 594, and 643 nm attributed to characteristic emissions of  ${}^4G_{5/2} \rightarrow {}^6H_J$  ( $J = 5/2, 7/2,$  and  $9/2$ ) transitions of Sm(III) [41].

### 3.5. Powder XRD patterns

Powder diffraction patterns of **1–4** are in agreement with those calculated on the basis of their structural data (figures S1–S4), which means complexes have been obtained as pure crystalline phases.

## 4. Conclusion

We have reported structures of four complexes generated from lanthanide salts and 2,2'-dimethyl-4,4'-bipyridine-*N,N'*-dioxide (L) [42,43]. In **1** and **2**, the  $\text{NO}_3^-$  coordinate with L, occupying six (five in **1**) sites and leaving the remaining sites available for N-oxide coordination, which lead to a rare 3-D three-fold interpenetrating **dia** framework (**1**) and polycatenation with a new  $\{8^2,10\}$  net (**2**). For **3** and **4**,  $\text{ClO}_4^-$  does not coordinate with Ln(III), which form a 3-D two-fold interpenetrating **dia** framework with large voids filled by  $\text{ClO}_4^-$ , L and water. Complex **3** shows strong luminescence in the solid state, which makes it a possible candidate for a new type of luminescent material.

### Supplementary material

Figures S1–S4 denote the PXRD patterns for **1–4**. Crystallographic data for the structures reported in this article have been deposited with the Cambridge Crystallographic Data Centre as Supplementary Publication No. CCDC-844345, CCDC-844346, CCDC-844347 and CCDC-844348 for **1–4**, respectively. Copies of the data can be obtained at <http://www.ccdc.cam.ac.uk/conts/retrieving.html> (or from the CCDC, 12 Union Road, Cambridge CB2 1EZ, UK; Fax: +44 1223336033; Email: [deposit@ccdc.cam.ac.uk](mailto:deposit@ccdc.cam.ac.uk)).

## Acknowledgements

This manuscript was financially supported by the scientific research foundation for the young scholars of Nanjing University of Information Science and Technology.

## References

- [1] J.L.C. Rowsell, O.M. Yaghi. *Angew. Chem. Int. Ed.*, **44**, 4670 (2005).
- [2] S. Kitagawa, R. Kitaura, S. Noro. *Angew. Chem. Int. Ed.*, **43**, 2334 (2004).
- [3] O.M. Yaghi, M. O'Keeffe, N.W. Ockwing, H.K. Chae, M. Eddaoudi, J. Kim. *Nature*, **423**, 705 (2003).
- [4] D. Maspoch, D. Ruiz-Molina, J. Veciana. *Chem. Soc. Rev.*, **36**, 770 (2007).
- [5] N.R. Champness, *J. Chem. Soc., Dalton Trans.* 877 (2006).
- [6] C. Kepert. *Chem. Commun.*, 695 (2006).
- [7] R.-Q. Zou, L. Jiang, H. Senoh, N. Takeichi, Q. Xu. *Chem. Commun.*, 3526 (2005).
- [8] X.D. Guo, G.S. Zhu, F.X. Sun, Z.Y. Li, X.J. Zhao, X.T. Li, H.C. Wang, S.L. Qiu. *Inorg. Chem.*, **45**, 2581 (2006).
- [9] C. Qin, X. Wang, E. Wang, Z. Su. *Inorg. Chem.*, **44**, 7122 (2005).
- [10] K.-L. Wong, G.-L. Law, Y.-Y. Yang, W.-T. Wong. *Adv. Mater.*, **18**, 1051 (2006).
- [11] W.-S. Liu, T.-Q. Jiao, Y.-Z. Li, Q.-Z. Liu, M.-Y. Tan, H. Wang, L.-F. Wang. *J. Am. Chem. Soc.*, **126**, 2280 (2004).
- [12] X.D. Guo, G.S. Zhu, Q.R. Fang, M. Xue, G. Tian, J.Y. Sun, X.T. Li, S.L. Qiu. *Inorg. Chem.*, **44**, 3850 (2004).
- [13] G. Mancino, A.J. Ferguson, A. Beeby, N.J. Long, T.S. Jones. *J. Am. Chem. Soc.*, **127**, 524 (2005).
- [14] M. Boca, M. Izakovic, G. Kickelbick, M. Valko, F. Renz, H. Fuess, K. Matuzsna. *Polyhedron*, **24**, 1913 (2005).
- [15] G. Poneti, K. Bernot, L. Bogani, A. Caneschi, R. Sessoli, W. Wernsdorfer, D. Gatteschi. *Chem. Commun.*, **1807**, (2007).
- [16] L.F. Ma, L.Y. Wang, M. Du, S.R. Batten. *Inorg. Chem.*, **49**, 365 (2010).
- [17] A. Mateo-Alonso, P. Brough, M. Prato. *Chem. Commun.*, **1412**, (2007).
- [18] J.H. Jia, A.J. Blake, N.R. Champness, P. Hubberstey, C. Wilson, M. Schröder. *Inorg. Chem.*, **47**, 8652 (2008).
- [19] N.R. Goud, N.J. Babu, A. Nangia. *Cryst. Growth Des.*, **11**, 1930 (2011).
- [20] D.B. Dang, Y. Bai, C. He, J. Wang, C.Y. Duan, J.Y. Niu. *Inorg. Chem.*, **49**, 1280 (2010).
- [21] D.L. Long, R.J. Hill, A.J. Blake, N.R. Champness, P. Hubberstey, D.M. Proserpio, C. Wilson, M. Schröder. *Angew. Chem. Int. Ed.*, **43**, 1851 (2004).
- [22] D.L. Long, A.J. Blake, N.R. Champness, C. Wilson, M. Schröder. *Angew. Chem. Int. Ed.*, **40**, 2443 (2001).
- [23] S.H. Bossmann, H. Duerr, M.R. Pokhrel. *Synthesis*, **6**, 907 (2005).
- [24] SAINT, Program for Data Extraction and Reduction, Bruker AXS, Inc.; Madison, WI, (2001).
- [25] G.M. Sheldrick. *SHELXS-97, Program for the Solution of Crystal Structures*, University of Göttingen, Göttingen (1997).
- [26] G.M. Sheldrick. *SHELXL-97, Program for Refinement of Crystal Structures*, University of Göttingen, Göttingen (1997).
- [27] M. Eddaoudi, D.B. Molar, H. Li, B. Chen, T.M. Reineke, M. O'Keeffe, O.M. Yaghi. *Acc. Chem. Res.*, **34**, 319 (2001).
- [28] B. Moulton, M.J. Zaworotko. *Chem. Rev.*, **101**, 1629 (2001).
- [29] S.R. Batten, B.F. Hoskins, R. Robson. *Chem. Eur. J.*, **6**, 156 (2000).
- [30] S. Noro, S. Kitagawa, M. Kondo, K. Seki. *Angew. Chem. Int. Ed.*, **39**, 2081 (2000).
- [31] S.R. Batten, R. Robson. *Angew. Chem. Int. Ed.*, **37**, 1460 (1998).
- [32] C.Y. Su, B.S. Kang, H.Q. Liu, Q.G. Wang, T.C.W. Mak. *Chem. Commun.*, **1551**, (1998).
- [33] T.M. Reineke, M. Eddaoudi, D. Molar, M. O'Keeffe, O.M. Yaghi. *J. Am. Chem. Soc.*, **122**, 4843 (2000).
- [34] S.R. Batten, R. Robson. *Angew. Chem. Int. Ed.*, **37**, 1461 (1998).
- [35] A.L. Spek. *PLATON, A Multipurpose Crystallographic Tool*, Utrecht University, Utrecht (2003).
- [36] Y.K. He, Z.B. Han. *Inorg. Chem. Commun.*, **10**, 1523 (2007).
- [37] J. Gregoliński, A. Kochel, J. Lisowski. *Polyhedron*, **25**, 2745 (2006).
- [38] H.S. Ra, K.M. Ok, P.S. Halasyamani. *J. Am. Chem. Soc.*, **125**, 7764 (2003).
- [39] J.S.O. Evans, S. Benard, P. Yu, R. Clement. *Chem. Mater.*, **13**, 3813 (2001).
- [40] L. Song, S.W. Du, J.D. Lin, H. Zhou, T. Li. *Cryst. Growth Des.*, **7**, 2268 (2007).
- [41] J.-W. Cheng, S.-T. Zheng, E. Ma, G.-Y. Yang. *Inorg. Chem.*, **46**, 10534 (2007).
- [42] H.-S. Wang, G.-C. Li, Y. Chen, Z.-J. Zhang, M.-L. Liu. *J. Coord. Chem.*, **63**, 4068 (2010).
- [43] J.-L. Wang, K.-L. Hou, Y.-H. Xing, Z.-Y. Deng, Z. Shi. *J. Coord. Chem.*, **64**, 3767 (2011).